to the surface. Fig. 2 shows three examples among K-NET stations. Black lines are separated HSAF and VSAF from the observed strong motions by GIT, while red lines are 1-D theoretical HSAF and VSAF. For theoretical calculations, we used boring data for upper 20m and J-SHIS data for the deeper part. The matching between the observation and the 1-D theory is quite good for HSAFs. The matching in VSAF is not as good as HSAF but still it is apparent to have significant VSAF in both the observation and the 1-D theory.

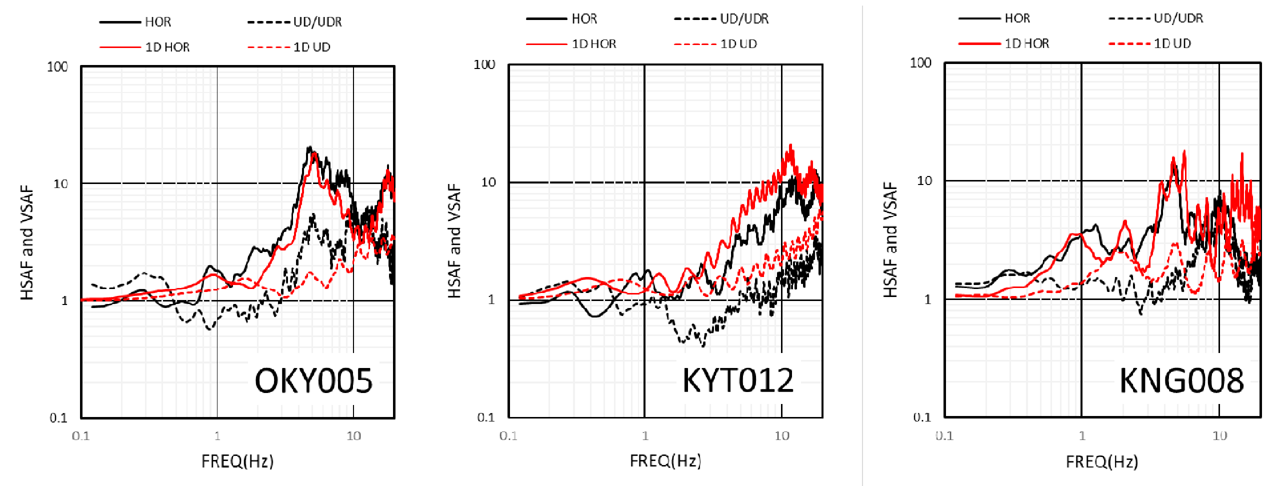

Fig. 2 – Comparisons of HSAFs and VSAFs in observation and theory.

3.2 V_BH_BR

We then address the vertical-to-horizontal spectral ratio V_BH_BR in the seismological bedrock. Fig. 3 shows, in a blue curve, the averaged ratio of the observed vertical spectral value with respect to the corrected horizontal spectral value as the outcrop motion equivalent to the seismological bedrock at the reference site (YMGH01), that is V_BH_BR. The figure shows that the ratio fluctuates gently around unity. In the range between 0.12 Hz and 20 Hz, the average minus one standard deviation is in good agreement with the square root of the ratio of S-wave velocity to P-wave velocity (red broken line) in the bedrock, which is expected from the diffuse wavefield theory in Eq. (3). As this value is about 0.8 in the case of a Poisson solid, it can be said that the vertical motion is nearly equal to the horizontal motion in the seismological bedrock.

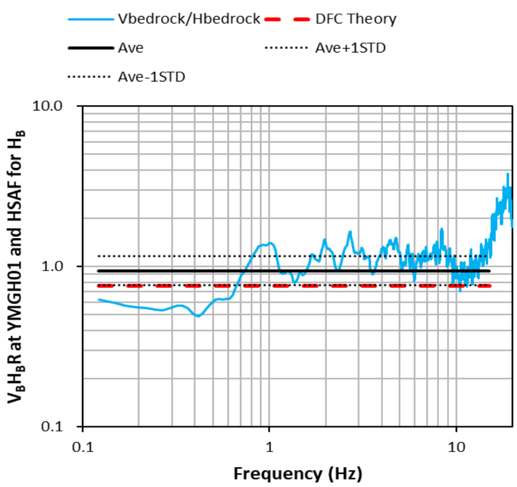

Fig. 3 – Comparison of V_BH_BR at the reference station YMGH01 with that of DFC theory.

3.3 VACF

We try to correct the EHVR by using the VSAF obtained by the simultaneous GIT analysis for both vertical and horizontal motions. Eq. (7) suggests that the correction through VSAF×VBHBR is necessary. Since the only constraint condition (reference point) in the GIT analysis of Nakano et al. (2015) [4] is the horizontal motion spectrum at the outcrop equivalent to the extracted seismological bedrock at YMGH01, the VACF in Eq. (8) is directly determined from the vertical site factors obtained by GIT. If the GIT analysis is conducted only for vertical motion, V_BH_BR should be corrected because the vertical motion at the reference point will be given as a norm in that case.

The 1,678 observation sites where ten or more seismic spectra were available were grouped into two groups divided by whether the peak amplitude of the EHVR was no less than 5 or less than 5. The sites were further classified into four categories according to different peak frequency ranges (1 Hz or less, between 1 Hz and 5 Hz, between 5 Hz and 10 Hz, and 10 Hz or more) to determine the average VACF for each category. The results are shown in Fig. 4a. The figure indicates that a) there are only negligible differences due to peak amplitude, b) there are relatively small differences due to peak frequency, c) the amount of correction increases as peak frequency decreases, and d) the correction amplitude is by a factor of about 3 at around 1 Hz and by a factor of 2.5 in the range between 1 Hz and 5 Hz. While the finding that spectra are not significantly affected by the characteristics of EHVR may appear unexpected given that the EHVR is correlated with both the P- and S-wave transfer functions, the similarity in the average characteristics of VACF does not necessarily mean that the P-wave velocity structure is similar throughout the nation. Nevertheless, it is evident that the fluctuation with frequency is smaller in the VSAF than in the HSAF as shown in Fig. 2.

Since the differences among the eight categories in Fig. 4a are relatively small, we calculated the average VACF of all sites without categorization for the sake of simplicity, which is shown in Fig. 4b. In the verification given below, we used this simple average VACF.

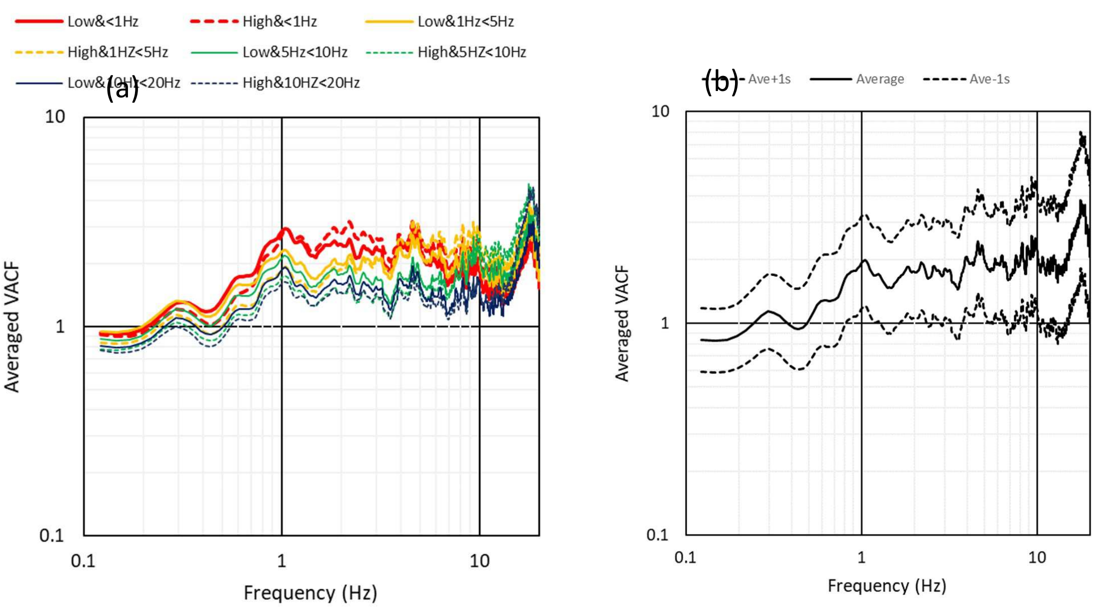

Fig 4 – Vertical Amplification Correction Function VACF (a) for eight categories based on the EHVR peak frequency and amplitude and (b) for all the 1,678 sites used.

3.4 Validation of the VACF method

We verified the capability of the proposed VACF method in reproducing the observed HSAF from the observed EHVR. While we have obtained average values (Fig. 4) by using the sites whose number of observed earthquakes was 10 or more, we have separately made a comparison using sites whose number of earthquakes was seven to nine, which have not been subjected to the aforementioned averaging. As shown in the eight examples given in Fig. 5, the HSAF obtained by the GIT was reproduced successfully even though

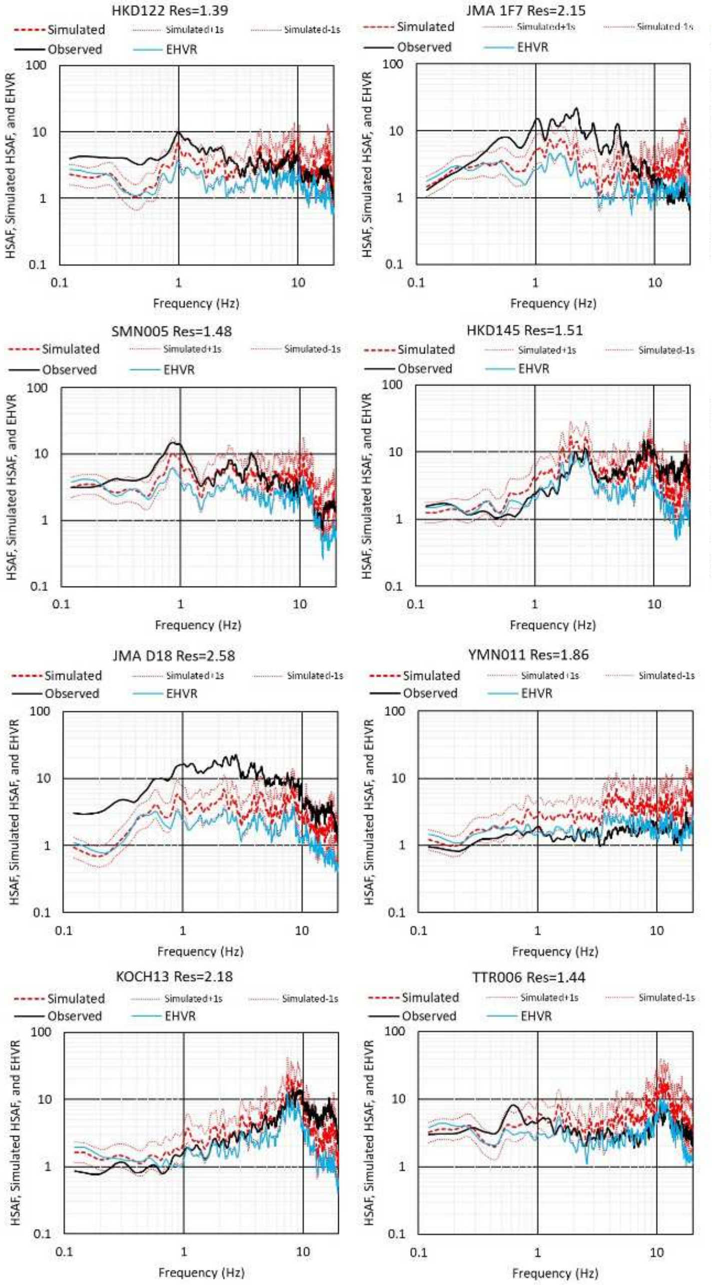

Fig. 5 – Comparison of the observed HSAF (black line) and the simulated HSAF (red broken line) obtained from the EHVR multiplied by the empirical VACF in Fig. 4b. The dotted lines represent the simulated HSAF using the average ± one standard deviation, and the thin blue line represents the EHVR used. “Res” in the header means the average residual (ratio) between observed and simulated.

a simple correction function in Fig.4b was used. Among these examples, the difference in estimation was particularly large at JMA D18 ("Res" in the figure is the average log-residual, which is the average spectral ratio), and this was because the actual VSAF was greater than the average at this site. As long as this method is used, it is inevitable that such sites will be found with a certain probability. When a conservative HSAF value is required, it is desirable to use the average correction function plus one standard deviation as a multiplication factor shown in Fig. 4b.

To grasp the average trend of our simulation results, we compared the simulated HSAF obtained by using the VACF (Fig. 4b) and the EHVR with the observed HSAF for a total of 103 sites whose numbers of observed earthquakes were seven to nine. We also compared the uncorrected EHVR directly with the HSAF (i.e., Nakamura method). Fig. 6 shows their maximum and average amplitudes (●: HSAF, ○: EHVR) on the left and right sides, respectively. Fig. 7 shows the average log-residuals of all frequencies (black bar: EHVR red bar: simulated HSAF). The average operation is performed in the frequency range from 0.1 Hz to 15 Hz. Note that the average of the log-residuals is reverted to a real number (ratio) with the power of 10,

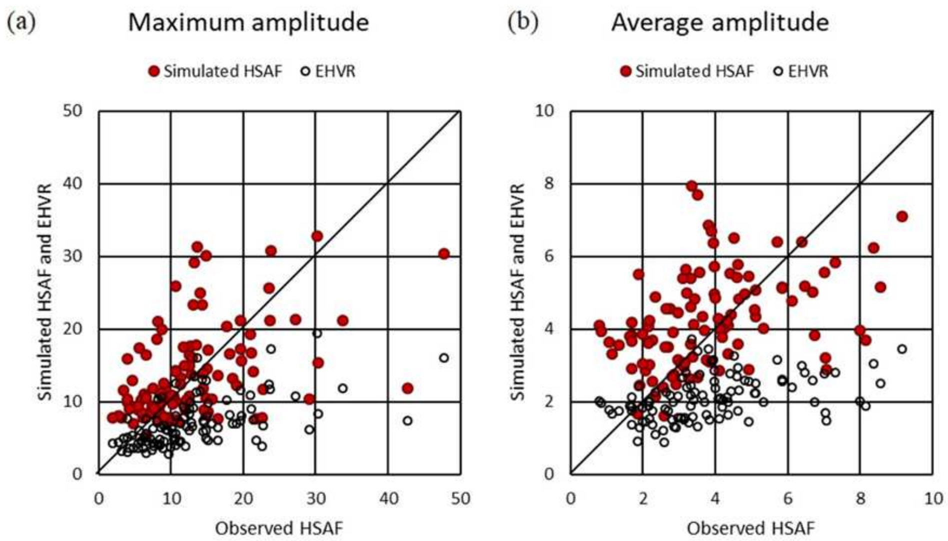

Fig. 6 – Comparison of the simulated HSAF or the EHVR (vertical axis) plotted against the observed HSAF (horizontal axis). (a) maximum amplitude, (b) average amplitude.

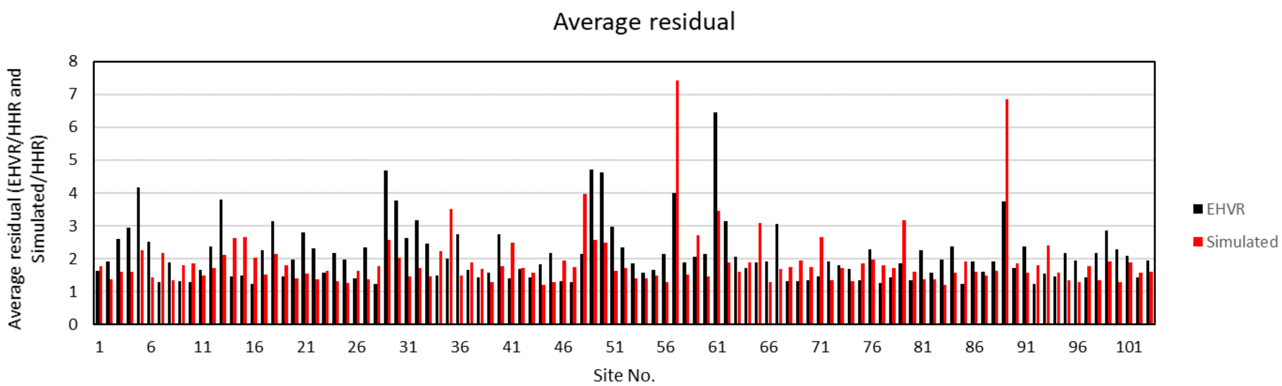

Fig. 7 – The averaged log-residuals between the observed EHVR and the observed HSAF (black bar), compared with the averaged log-residuals between the simulated HSAF and the observed HSAF (red bar). Two sites with extraordinary high residuals in the simulated HSAF are the sites of the JMA network, namely BE9 and D03, where significant attenuation in high-frequency range was found in both HSAFs and VSAFs.

meaning perfect matching when the ratio is unity. Whereas amplitude was obviously underestimated in the EHVR, data points became more closely distributed around the line of 1:1 after the correction. The log-residual data also indicates the improvement of matching in more than 60% of the sites. More than half of the remaining sites had small residuals in both the EHVR and the simulated HSAF, and the percentage of sites in which errors increased significantly after the correction was only about 10%. We found that the amplitudes of both the observed HSAF and VSAF in the high-frequency range are abnormally smaller than the average value in Fig. 7 at those sites where the degrees of matching are worsened after the correction, such as JMA BE9 and JMA D03. These sites may be under special conditions, and this is a subject of future investigation.

4. Conclusions

We proposed a simple method to deduce the horizontal site amplification factor (HSAF) in the main S-wave portion directly from the EHVR of observed earthquake ground motion. In this method, we have formulated a correction procedure based on the diffuse field theory; focused on observation records from 1,678 sites where ten or more earthquakes have been observed in the strong-motion networks K-NET, KiK-net, and JMA seismic intensity network; used the generalized spectral inversion technique (GIT) to determine the vertical site amplification factor (VSAF, to be precise, VSAF multiplied by V_BH_BR); and then averaged it to obtain the empirical vertical amplification correction function (VACF). The findings obtained are as follows:

1) The vertical-to-horizontal spectral ratio at the reference observation site (V_BH_BR) was nearly unity and agreed with the theoretical solution within the range of variation.

2) The amplitude of the VSAF, on average, was 30% to 40% of the HSAF obtained by GIT and the EHVR was obviously smaller than the HSAF by the amount of VSAF. Using the EHVR with no correction in place of the HSAF as proposed by Nakamura (1989) [5] will result in underestimation of HSAF.

3) It was possible to obtain the VACF on a very stable basis by reading out the peak amplitude and peak frequency of EHVR at each site and averaging the data in the corresponding category; there were only negligible differences due to peak amplitude; there were relatively small differences due to peak frequency; the amount of correction increased as the peak frequency decreased; and the VACF was the largest when EHVR peak frequency was 1 Hz or less, where the factor of about 3 was needed.

4) For the validation exercise of applicability, we applied the obtained VACF to 103 sites whose number of observed earthquakes was seven to nine so that they have not been used in the averaging. As a result, the observed HSAF has been successfully reproduced in about 90% of the sites, although some other sites have shown nearly doubled differences.

In summary, this paper proposed a new simple method, in which the main S-wave portion of earthquake ground motion is extracted, the average horizontal-to-vertical spectral ratio of this portion is determined, and this ratio is multiplied by the empirical correction function (VACF) to obtain the horizontal S-wave site amplification factor. Although this method inevitably entails errors in the VACF estimation due to site-specific characteristics, it is capable of evaluating the site effects of S-waves based on observed values in a wide frequency range from 0.1 Hz to 15 Hz. It should be noted that the proposed method obtains the horizontal S-wave amplification factor from the seismological bedrock, rather than the engineering bedrock, to the ground surface. For the sake of reliability, it is advisable to determine the average horizontal-to-vertical ratio of at least about 10 earthquakes.

5. Acknowledgments

A part of this study was supported by the JSPS Kakenhi Grant-in-Aid for Basic Research (A) No.26242034 and Grant-in-Aid for Basic Research (B) No.19H02405. Information provided by and discussions done with Profs. Pierre-Yves Bard, Cecile Cornou, and Alan Yong were highly appreciated.

References

[1] Andrews, D.J. (1986): Objective determination of source parameters and similarity of earthquakes of different size, *Earthquake Source Mechanics* (eds. S. Das, J. Boatwright and C. H. Scholz), American Geophysical Union, Washington, D.C., 1986. doi: 10.1029/GM037p0259.

[2] Kawase, H. and H. Matsuo (2004): Amplification characteristics of K-NET, KiK-NET, and JMA Shindokei network sites based on the spectral inversion technique, *13th World Conf. on Earthquake Engineering*, Vancouver, Canada, Paper No. 454.

[3] Kawase, H. (2006): Site effects derived from spectral inversion method for K-NET, KiK-net, and JMA strong-motion network with special reference to soil nonlinearity in high PGA records, *Bull. Earthq. Res. Inst.*, Tokyo Univ. 81, 309–315.

[4] Nakano, K., S. Matsushima, and H. Kawase (2015): Statistical properties of strong ground motions from the generalized spectral inversion of data observed by K-NET, KiK-net, and the JMA Shindokei Network in Japan, *Bull. Seism. Soc. Am*., 105: 2662-2680, doi:10.1785/0120140349.

[5] Nakamura Y. (1989): A method for dynamic characteristics estimation of subsurface using microtremor on the ground surface, *Railway Tech. Res. Inst.*, Q. Rep. 30(1): 25-30

[6] Kawase, H., Y. Mori, and F. Nagashima (2017): Difference of horizontal-to-vertical spectral ratios of observed earthquakes and microtremors and its application to S-wave velocity inversion based on the diffuse field concept, *Earth, Planets and Space*, Vol.70, No.1, Open Access, doi: 10.1186/s40623-017-0766-4.

[7] Kawase, H., F. Nagashima, K. Nakano, and Y. Mori (2018): Direct evaluation of S-wave amplification factors from microtremor H/V ratios: Double empirical corrections to "Nakamura" method, *Soil Dyn. Earthquake Eng.*, Open Access, doi: 10.1016/j.soildyn.2018.01.049.

[8] Kawase H., F.J. Sánchez-Sesma, and S. Matsushima (2011): The optimal use of horizontal-to-vertical spectral ratios of earthquake motions for velocity inversions based on diffuse-field theory for plane waves. *Bull. Seism. Soc. Am.*, 101, 2011-2014.

